Electronic Supplementary Material (ESI) for Catalysis Science & Technology.
This journal is © The Royal Society of Chemistry 2018

Supplementary Information

Table S1. Kinetic constants using first-order kinetic model for photocatalytic reduction of Cr (VI) and photocatalytic degradation of dimethoate over different photocatalysts.

		$g\text{-}C_3N_4$	$C/g\text{-}C_3N_4$	$\alpha\text{-}Fe_3O_4/C/g\text{-}C_3N_4$
Cr(VI)	k_{obs} / min^{-1}	0.0017	0.0109	0.0355
	(Adj-r^2)	(0.99)	(0.99)	(0.97)
Dimethoate	k_{obs} / min^{-1}	0.0095	0.0112	0.0203
	(Adj-r^2)	(0.99)	(0.99)	(0.98)

Table S2. The values of fitted PL lifetime τ_i and corresponding constant A_i of $g\text{-}C_3N_4$, $C/g\text{-}C_3N_4$, and $Fe_3O_4/C/g\text{-}C_3N_4$, respectively.

	τ_1 / ns (A_1)	τ_2 / ns (A_2)	τ_3 / ns (A_3)	$\langle\tau\rangle$ / ns	χ^2
$g\text{-}C_3N_4$	1.55 (1362.2)	4.91 (565.0)	21.57 (86.8)	8.48	0.927
$C/g\text{-}C_3N_4$	1.33 (1630.1)	4.59 (434.0)	18.75 (47.36)	5.68	0.902
$Fe_3O_4/C/g\text{-}C_3N_4$	1.27 (1640.0)	4.08 (429.2)	15.53 (54.22)	4.89	0.943

*The photoluminescence decays were fit to Eq. (S1) as three exponentials using the PicoQuant software (Fluofit, PicoQuant) so that the lifetimes (τ_i) and the pre-exponential factors (A_i) were determined. The value of χ^2, as well as visual inspection

of the residuals were used to determine how well the calculated decay fitted the experimental data. Fits were considered acceptable when the χ^2 value was between 0.9 and 1.1. The intensity-average lifetime of the emission decay is calculated by Eq. (S2).

$$I(t) = I_0 \sum_{1}^{i} A_1 e^{-t/\tau_i} \quad \text{(S1)}$$

$$< \tau >= \frac{A_1\tau_1^2 + A_2\tau_2^2 + A_3\tau_3^2}{A_1\tau_1 + A_2\tau_2 + A_3\tau_3} \quad \text{(S2)}$$

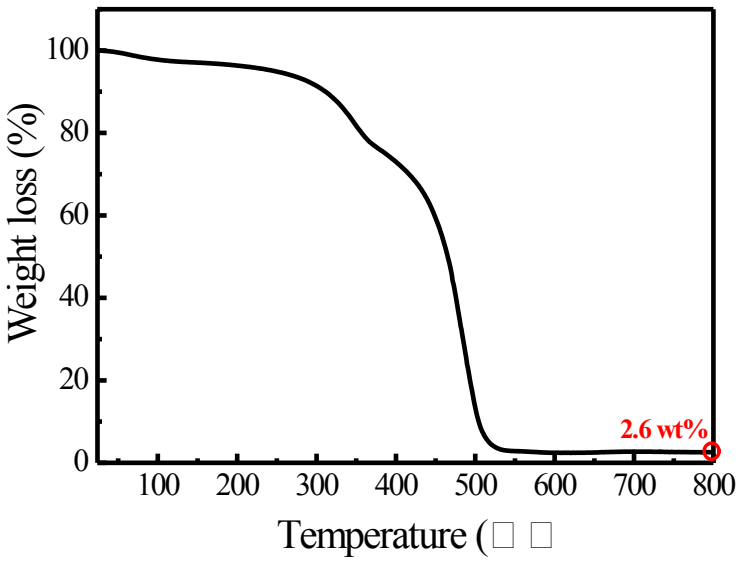

Figure S1. Thermogravimetric curve of Fe_3O_4/C/g-C_3N_4.

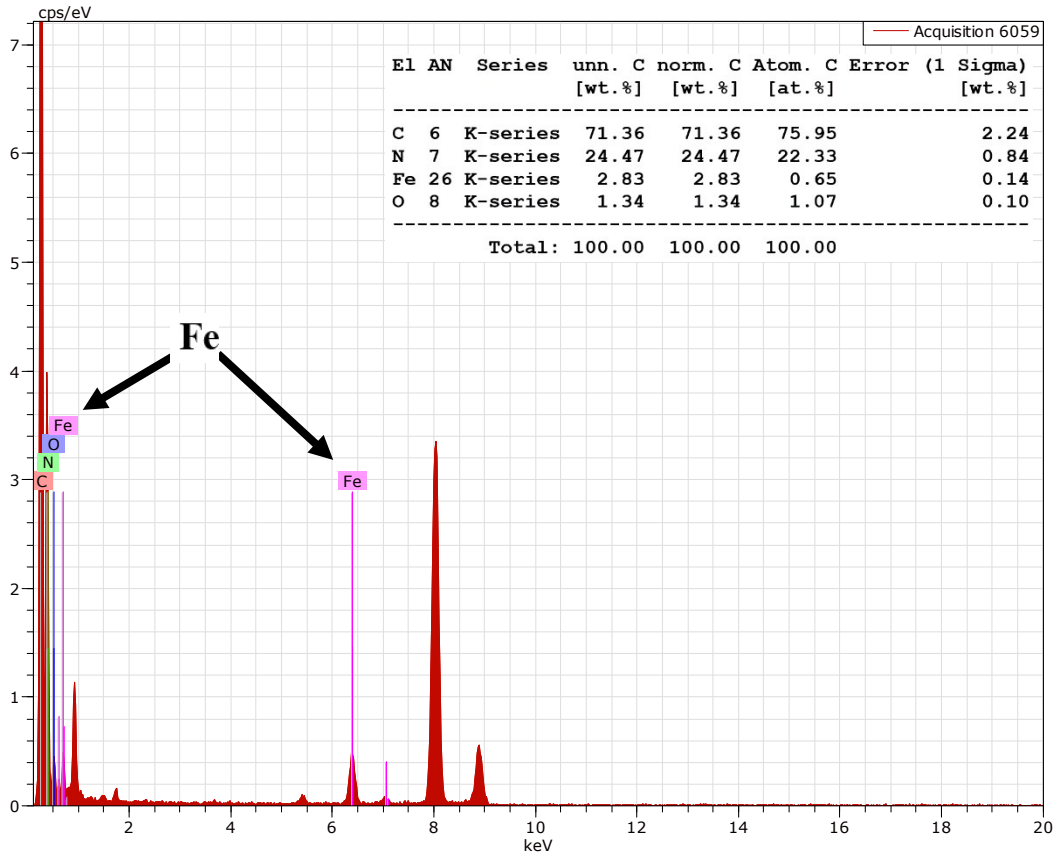

Figure S2. Elemental proportion in α-Fe_3O_4/C/g-C_3N_4 from EDS elemental analysis.

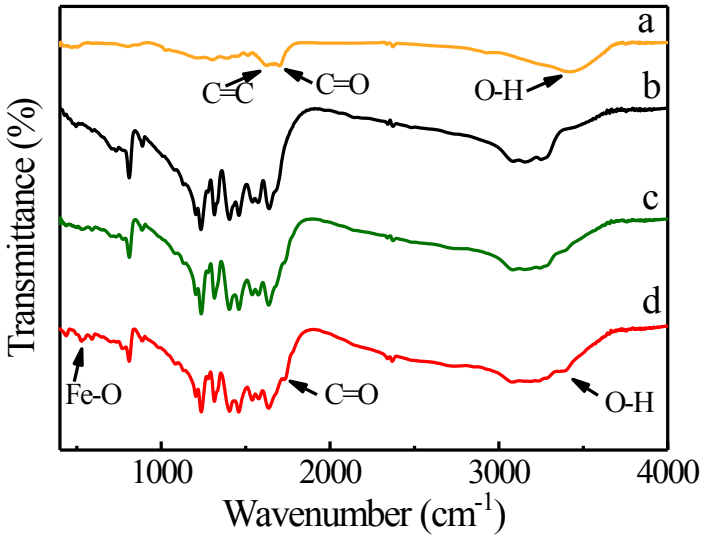

Figure S3. FTIR of carbon (a), g-C_3N_4 (b), C/g-C_3N_4 (c) and Fe_3O_4/C/g-C_3N_4 (d).

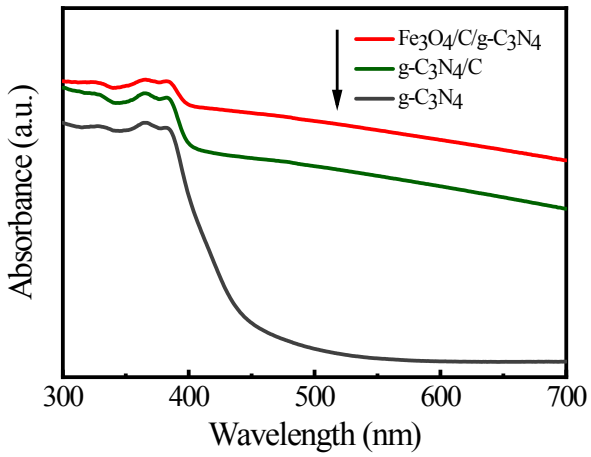

Figure S4. UV-vis diffuse reflectance spectra of Fe_3O_4/C/g-C_3N_4, C/g-C_3N_4, and g-C_3N_4.

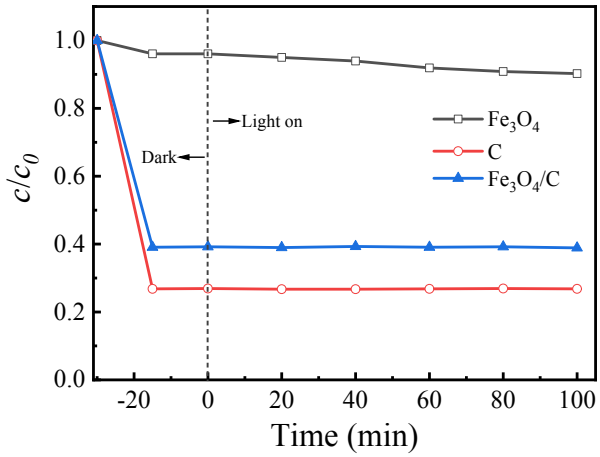

Figure S5. Absorption and photoreduction of Cr (VI) (20 mg/L) by Fe_3O_4, carbon, and Fe_3O_4/C (0.2 g/L) under visible light irradiation (λ≥420 nm), respectively.

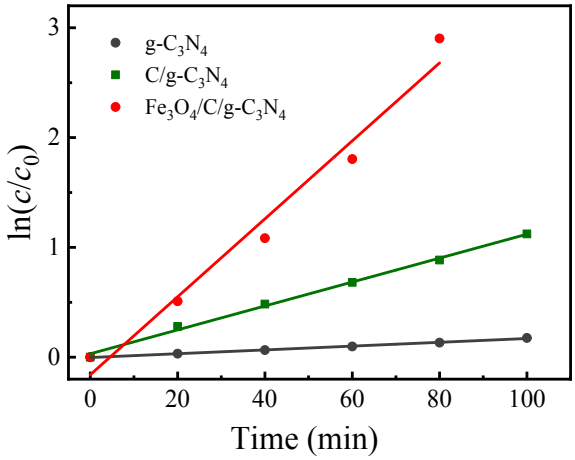

Figure S6. Kinetic fit of the photoreduction of Cr (VI) (20 mg/L) by g-C_3N_4, C/g-C_3N_4, and Fe_3O_4/C/g-C_3N_4 (0.2 g/L), respectively, to the first-order kinetic model under visible light irradiation (λ≥420 nm).

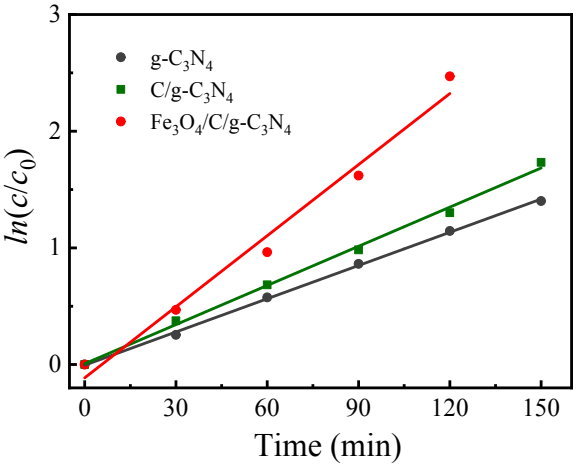

Figure S7. Kinetic fit of photodegradation of dimethoate (10 mg/L) by g-C_3N_4, C/g-C_3N_4, and Fe_3O_4/C/g-C_3N_4 (0.2 g/L) to first-order kinetic model under visible light irradiation (λ≥420 nm), respectively.

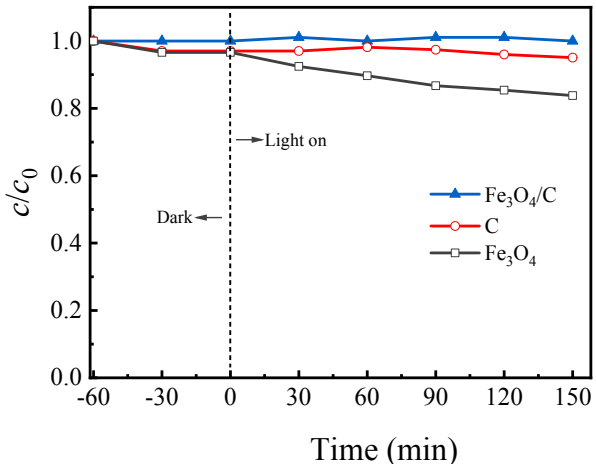

Figure S8. Absorption and photodegradation of dimethoate (10 mg/L) by Fe_3O_4, carbon, and Fe_3O_4/C (0.2 g/L) under visible light irradiation ($\lambda \geq 420$ nm), respectively.

Figure S9. The magnetic separation for possessing the Fe_3O_4 component.

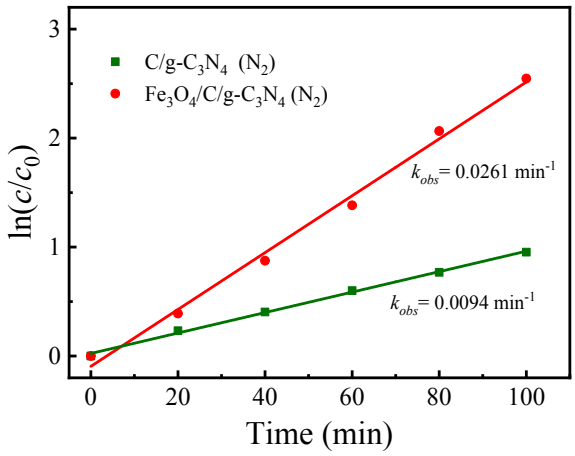

Figure S10. Kinetic fit of the photoreduction of Cr(VI) (20 mg/L) by C/g-C_3N_4 or Fe_3O_4/C/g-C_3N_4 (0.2 g/L) to first-order kinetic mode under the visible light irradiation ($\lambda \geqslant 420$ nm) with the continual N_2 purging into the solution.

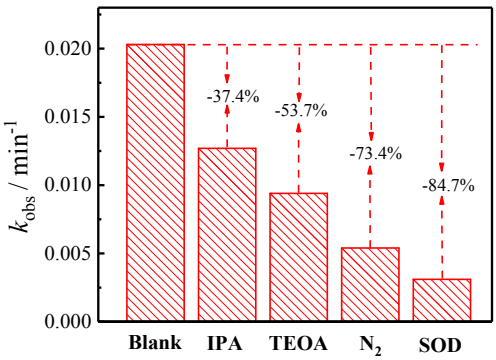

Figure. S11 Kinetic constants for photocatalytic degradation of dimethoate (10 mg/L) over Fe_3O_4/C/g-C_3N_4 (0.2 g/L) with N_2 continually purged and different scavengers (IPA, 0.01ml; TEOA, 0.01ml; SOD, 1mg) added into the 50ml reaction mixture, respectively.